# ANALYSIS OF AXIAL DAMPING IN

# SEGMENTED CONSTRAINED LAYER

# FIBROUS COMPOSITES

by

Alan M. Carver

A thesis submitted in partial fulfillment
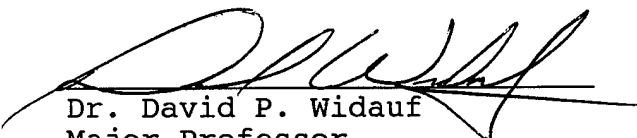of the requirements for the degree

of

MASTER OF SCIENCE

in

Industrial Technology
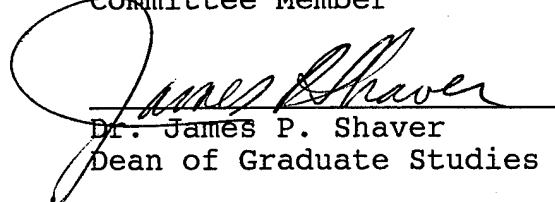
Approved:

_____
Dr. David P. Widauf
Major Professor

_____
Dr. Charles E. Tinney
Committee Member

_____
Dr. Thomas H. Fronk
Committee Member

_____
Dr. James P. Shaver
Dean of Graduate Studies

UTAH STATE UNIVERSITY
Logan, Utah

1995

| 1. AGENCY USE ONLY (Leave blank) | 2. REPORT DATE June 1995 | 3. REPORT TYPE AND DATES COVERED |
|---|---|---|

| 4. TITLE AND SUBTITLE Analysis of Axial Damping In Segmented Constrained Layer Fibrous Composites | 5. FUNDING NUMBERS |
|---|---|

**6. AUTHOR(S)**

Alan M. Carver

| 7. PERFORMING ORGANIZATION NAME(S) AND ADDRESS(ES) AFIT Students Attending: Utah State University | 8. PERFORMING ORGANIZATION REPORT NUMBER AFIT/CI/CIA 95-049 |
|---|---|

| 9. SPONSORING/MONITORING AGENCY NAME(S) AND ADDRESS(ES) DEPARTNEMT OF THE AIR FORCE AFIT/CI 2950 P STREET, BDLG 125 WRIGHT-PATTERSON AFB OH 45433-7765 | 10. SPONSORING/MONITORING AGENCY REPORT NUMBER |
|---|---|

**11. SUPPLEMENTARY NOTES**

| 12a. DISTRIBUTION/AVAILABILITY STATEMENT Approved for Public Release IAW AFR 190-1 Distribution Unlimited BRIAN D. GAUTHIER, MSgt, USAF Chief Administration | 12b. DISTRIBUTION CODE |
|---|---|

**13. ABSTRACT (Maximum 200 words)**

DTIC
SELECTED
JUL 14 1995
B

DTIC QUALITY INSPECTED 5

| 14. SUBJECT TERMS | | 15. NUMBER OF PAGES 63 |
|---|---|---|
| | | 16. PRICE CODE |

| 17. SECURITY CLASSIFICATION OF REPORT | 18. SECURITY CLASSIFICATION OF THIS PAGE | 19. SECURITY CLASSIFICATION OF ABSTRACT | 20. LIMITATION OF ABSTRACT |
|---|---|---|---|

# ABSTRACT

Analysis of Axial Damping in

Segmented Constrained Layer

Fibrous Composites

by

Alan M. Carver, Master of Science

Utah State University, 1995

Major Professor:  David P. Widauf
Department:  Industrial Technology and Education

The axial damping in segmented ply specimens is compared with that of continuous ply specimens.  Axial damping increases in both designs as the free-edge transverse shear becomes more important.  The axial damping of segmented specimens surpasses that of the unsegmented design when small segment aspect ratios are employed.  This observed trend corresponds with earlier finite element models but fails to reach magnitudes considered practically important.  Theories are presented concerning the role of damping mechanisms and techniques are suggested for improving axial damping without segmenting the plies.

(72 pages)

## ACKNOWLEDGMENTS

CONTENTS

LIST OF TABLES

LIST OF FIGURES

CHAPTER 1

THE PROBLEM AND ITS SETTING

Introduction

Passive damping refers to the ability of a structure to
dissipate vibrations based on its material properties and
geometry.  Rubber and other viscoelastic materials have long
been combined with stiff materials such as steel to create
damping in the final structure.  Generally this is done by
sandwiching viscoelastic materials between load-bearing
stiff materials.  When these constraining layers are
displaced, the viscoelastic material is stressed and a
portion of the load energy is dissipated.  This method works
well for bending loads, but since axial loads produce little
displacement, axial damping has been difficult to achieve.

Some improvement has been attained by using fibrous
composites as constraining layers and tailoring them toward
more displacement under axial loads.  This is done by
constraining the viscoelastic layer between laminates of
opposing fiber angles.  When loaded axially, the fibers
attempt to align with the load and cause the laminates to
scissor against each other. The resulting shear stress is
absorbed and dampened in the viscoelastic layer.

Recently efforts have been made to improve this design
by alternating the fiber direction within each ply. It was
thought that this would cause even greater distortion in the
viscoelastic layer and therefore improve damping.

The purpose of this thesis is to better understand the mechanisms responsible for damping in these constrained layer fibrous composites. Specimens of both designs are tested and the results compared.

## Problem Statement

This study will compare axial damping in selected segmented ply specimens and similar constrained layer specimens to better understand the mechanisms of transverse shear in fibrous damping composites.

## Subproblems

1. To analyze the axial damping abilities of selected segmented ply specimens and investigate the mechanisms of transverse shear.

2. To analyze the axial damping abilities of selected constrained layer specimens and investigate the mechanisms of transverse shear.

3. To learn what a comparative study of these two analyses reveals about the mechanisms of transverse shear in fibrous damping composites.

## Assumptions

1. Damping ability can be measured.

2. The samples studied represent the entire population of similar structures.

## Definition of Terms

1.  <u>Dynamic Signal Analyzer</u>:  An instrument that can graph vibrations as magnitude in decibels versus frequency in Hertz.  This instrument receives its input from an accelerometer mounted to the specimen being studied.  The dynamic system analyzer used in this study is a Hewlett Packard 3560A.

2.  <u>Constrained Layer Construction</u>:  For the purposes of this thesis, constrained layer construction will refer to a composite in which a viscoelastic layer is constrained between continuous fiber laminates of opposing fiber angles as shown in Figure 1.
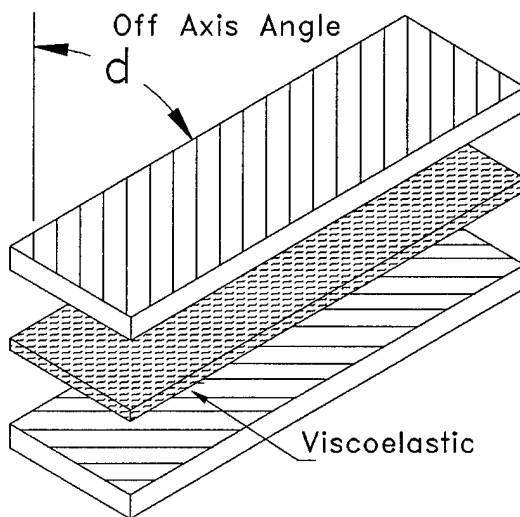


<u>Figure 1</u>.  Constrained layer construction.

3.  <u>Segmented Ply Construction</u>:  Similar to constrained layer construction except that the fibers are cut within each ply and alternated at plus and minus orientation angles to produce a V-shape or chevron pattern as shown in Figure 2.



Viscoelastic
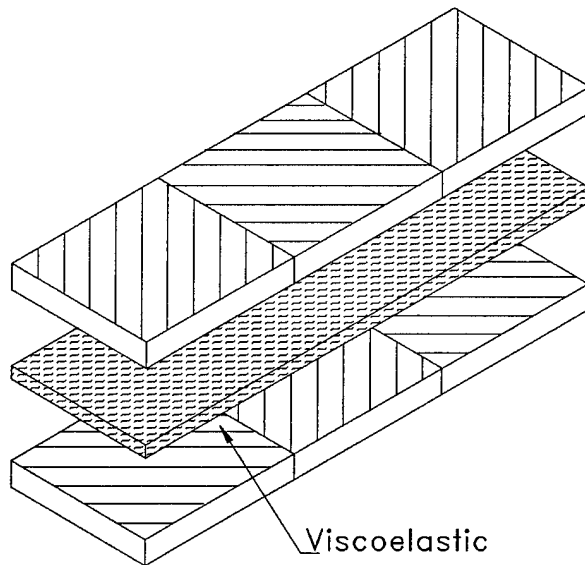
<u>Figure 2</u>.  Segmented ply construction.

CHAPTER 2

REVIEW OF RELATED LITERATURE

Introduction

Passive damping refers to the damping ability of a structure based on its material properties and geometry. Active damping is achieved with sensors and actuators that detect vibrations and then counter them with appropriate out-of-phase vibrations.

Constrained layer damping, by far the most common form of passive damping, is achieved by constraining a viscoelastic material between two rigid plates. The plates provide the necessary structural stiffness while the viscoelastic material absorbs vibrations and dissipates them as heat.

In 1939 the first patent involving constrained layer damping systems was issued. Now 55 years later, damping finally is understood well enough that it has become an accepted design alternative. Breakthroughs in computer technology, new materials, and more widespread standardization of material data stand out as the prime contributors in making damping an important design consideration. More than any other factor, the use of finite element analysis has encouraged the more general use of damping systems (Drake, 1985).

# Review

Fibrous composites already possess damping abilities by nature of the polymer resins that bind their fibers. Several studies have been conducted to investigate the damping effect of different matrix and fiber properties. Sun, Gibson, and Chaturvedi (1985) investigated the role of fiber length and diameter on laminate damping. They (e.g., Sun et al., 1985) identified a relationship between fiber aspect ratio and damping within certain frequency ranges. Of greatest interest, though, is their discovery that orienting the fibers off-axis produced more damping than varying fiber aspect ratios. Suarez and Gibson (1986) confirmed that fiber orientation, and specifically off-axis orientation, was a better approach to damping than varying the fiber aspect ratio. By building upon these studies, further research focused on describing the mechanisms at work and optimizing the off-axis damping angle. The idea that the fibers were slipping inside the resin matrix, thereby dissipating energy through friction and heat, was reinforced when it was observed that damping increased with broken fibers (Saravanos & Chamis, 1989). Interlaminar friction caused by shear coupling was also suspected to contribute to damping. Suarez and Gibson (1986) determined that shear coupling damping effects existed between angles of 5 and 30 degrees with the contribution decreasing

progressively after 30 degrees.

Combining the natural damping and tailorability of composites with a constrained layer design was the obvious next step and has met with favorable results. Some improvements have even been realized in the area of axial damping. The scissoring action of reverse angle constraining layers provides damping for axial loads, whereas conventional constrained layer designs were only effective with transverse or bending loads.

In an attempt to maximize the benefits of this scissoring action, researchers have begun investigating a segmented constrained layer design. In this design the fiber angles are reversed within the constraining layer and also above and below the viscoelastic. Dolgin (1990) first suggested this design of alternating the off-axis pattern. In his patent application, he termed the design a V-shape or chevron pattern with multiple sections. Olcott (1992) carried out some limited testing and analysis of this design using circular tubes and "I" beams as test geometries. Olcotts' results suggested improved axial damping could be achieved with the V-shape or chevron pattern. Further investigation of this design was carried out by Fronk (Fronk, Womack, Ellis, & Finlinson, in press), utilizing finite element analysis. Fronk (Fronk et al., in press) compared several different computer models representing flat specimens of various geometries. The damping mechanisms of

both chevron pattern and continuous fiber constrained layer designs were compared.  Fronk et al. determined that for certain geometries the segmented constrained layer design could outdampen the normal constrained layer design.  Specifically they reported that as the segment length-to-width ratio decreased, the chevron pattern's damping ability increased.  This increase continued until it surpassed that of the constrained layer design at an aspect ratio of approximately 2.

## Summary

Gibson (1994) has stated that with more and more stringent requirements for performance and precision being placed on structures and machines, damping is becoming an essential design consideration.  The advent of finite element analysis has enabled designers to improve the basic constrained layer design and preliminary studies have pointed to segmenting and reversing the fiber plies as a means to increasing axial damping.

# CHAPTER 3

## RESEARCH METHODOLOGY

### Overview

Two experiments were conducted that compared impulse frequency responses from segmented ply specimens with those of constrained layer specimens. The specimens were all constructed of 12 plies of AKZO Fortafil 3(c) graphite epoxy prepreg separated into three layers of four plies by two layers of Avery Dennison laminating adhesive.

In the first experiment the effect of segment aspect ratio or segment length-to-width ratio was investigated by testing specimens 6 inches long with widths of 1, 2, and 3 inches. The segmented specimens all had three segments and viscoelastic layers .010 inches thick.

The second experiment studied the effect of different segment aspect ratios by testing specimens with the same length and width but different numbers of segments. The specimens were 9 inches long and 3 inches wide with viscoelastic layers .005 inches thick. Segmented specimens were constructed with two, three, and four segments.

Testing was conducted using a Hewlett Packard 3560A Dynamic Signal Analyzer, a piezoelectric accelerometer, gain controllers, and a modally tuned hammer. The specimens were suspended by two nylon lines and the accelerometer was attached to one end with beeswax (see Figure 3). The

specimens were tapped with the hammer on the end opposite

the accelerometer, and the HP 3560A analyzed the

accelerometer output and produced frequency response traces.

Three traces from each specimen were saved and analyzed.  A

sample trace from each specimen can be seen in Appendix D.
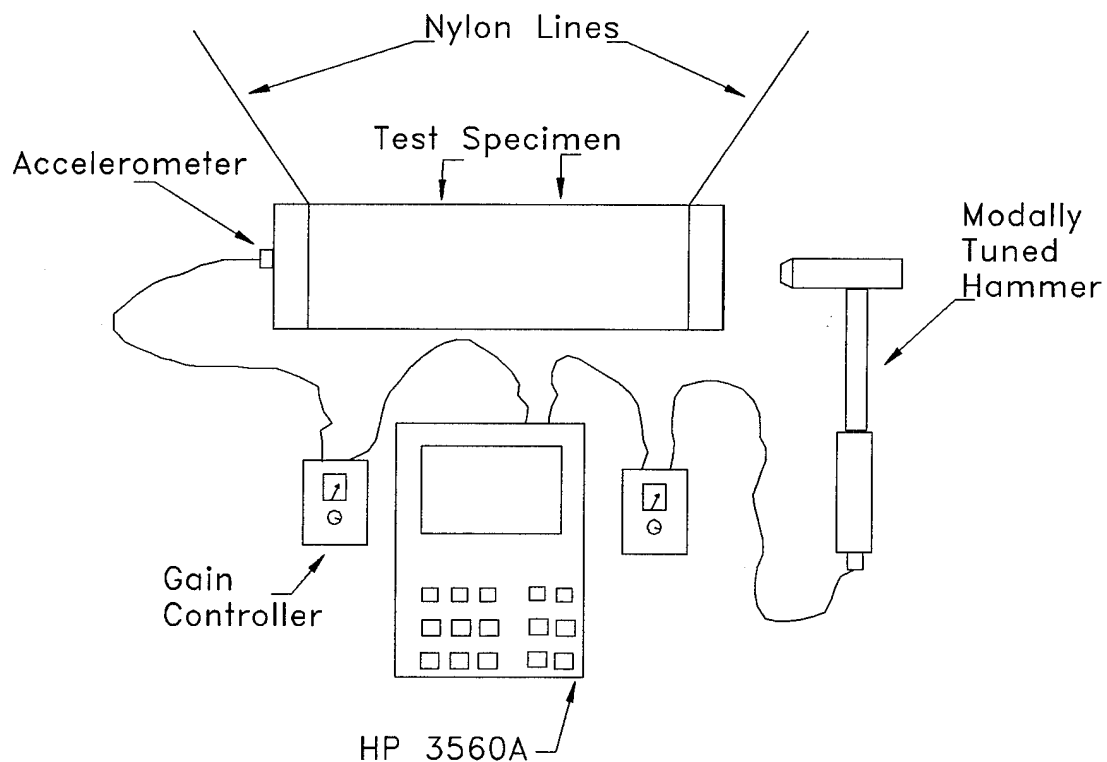


Figure 3.  Test apparatus and setup.

Loss factors were derived for each specimen using the equation

$$\eta = \frac{\omega_2 - \omega_1}{\omega_0} \qquad (1)$$

where $\eta$ is the loss factor, $\omega_0$ is the peak or natural frequency, $\omega_1$ is the frequency 3 decibels to the left of the peak, and $\omega_2$ is the frequency 3 decibels to the right of the peak. Figure 4 shows how these values are taken from a frequency trace (Suarez, Gibson, Sun, & Debold, 1984).
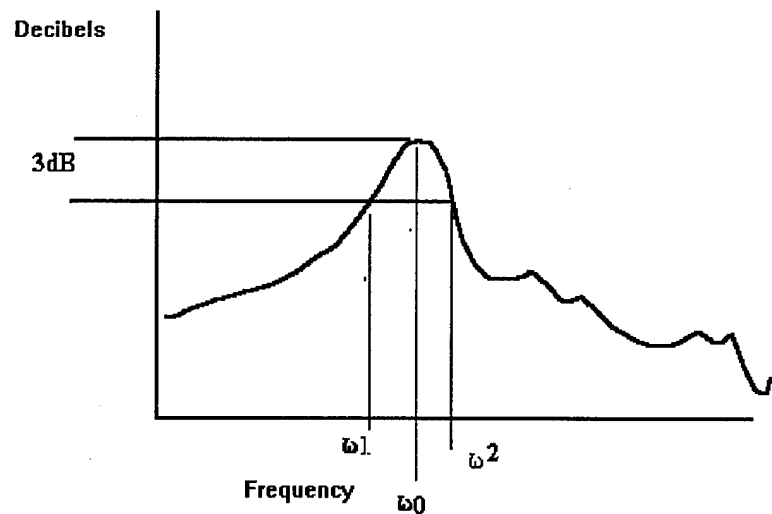


Figure 4. Three-decibel method for determining loss factor.

The loss factors from all the specimens were analyzed and compared.  The effect of segment aspect ratio was studied and the practical benefits of segmented ply construction versus constrained layer construction were considered.

## Experimental Design

The first experiment was a randomized block design with five blocks (oven batches), two construction types (segmented or constrained), and three widths.  Specimens were 6 inches long with widths of 1, 2, and 3 inches. Figure 5 shows how each oven batch consisted of six specimens representing the segmented ply construction and the constrained layer construction in each width.
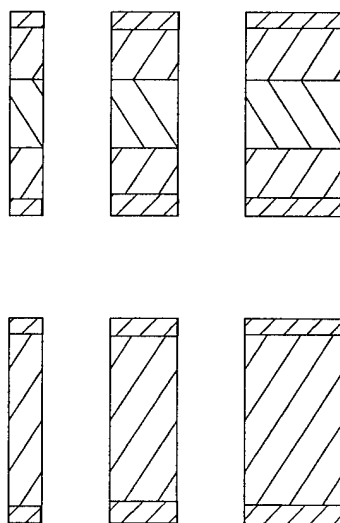


Figure 5.  1", 2", and 3" samples of both designs.

The experiment was blocked in this manner to reduce any variability that might have been introduced from one batch to the next. Variability arises due to subtle changes in the oven runs, the prepreg or viscoelastic material properties, and the environmental conditions present during manufacture.

Five batches were made for a total of 30 specimens or 15 constrained layer specimens and 15 segmented ply specimens. The second experiment varied the segment aspect ratio by leaving the overall dimensions constant and changing the number of segments. Segmented ply and constrained layer specimens were constructed 9 inches long and 3 inches wide. Segmented ply specimens were constructed with two, three, and four segments. Each specimen type was replicated four times for a total of 16 samples. The constrained layer specimens and the two- and three-segment specimens were all made together and cured in the same oven batch. The four-segment specimens were constructed later. This was considered acceptable after analysis of the first experiment revealed little variation between oven runs.

The viscoelastic layers in the second experiment were reduced to half the thickness of the first experiment. It was hoped that using less viscoelastic material would produce more pronounced differences in axial damping between the different designs.

Test Specimen Construction

All test specimens were made from .0056-inch AKZO Fortafil 3(c) graphite prepreg and .005-inch Avery Dennison laminating adhesive. The specimens for the first experiment were made from 12 plies of prepreg separated into three layers of four plies each by two layers of viscoelastic material, which consisted of two plies of laminating adhesive each. Figure 6 shows an exploded orthographic view of the segmented constraining layers depicting how the fiber angles were reversed within layers and on either side of the viscoelastic.
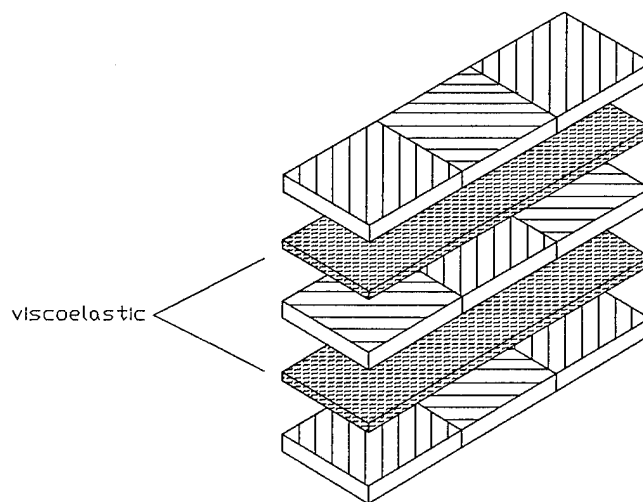


Figure 6. Experiment #1 segmented construction.

Figure 7 shows a cross section of the segmented ply construction displaying how lap joints were used to produce structural integrity in the composite. Lap joints for both experiments were a quarter-inch long.

In the first experiment specimens were 6 inches long with widths of 1, 2, and 3 inches. The fiber plies were oriented at plus or minus 18 degrees off-axis. The off-axis angle was chosen based on the estimated location of shear coupling maximums (see Appendix B). Each specimen was also constructed with endcaps made of 14 plies of graphite prepreg cut into quarter-inch strips. These small strips were co-cured at both ends and on both sides of the specimens to provide an attachment point for the accelerometer and a striking area for the hammer. The

viscoelastic

viscoelastic

positive anlge          negative angle
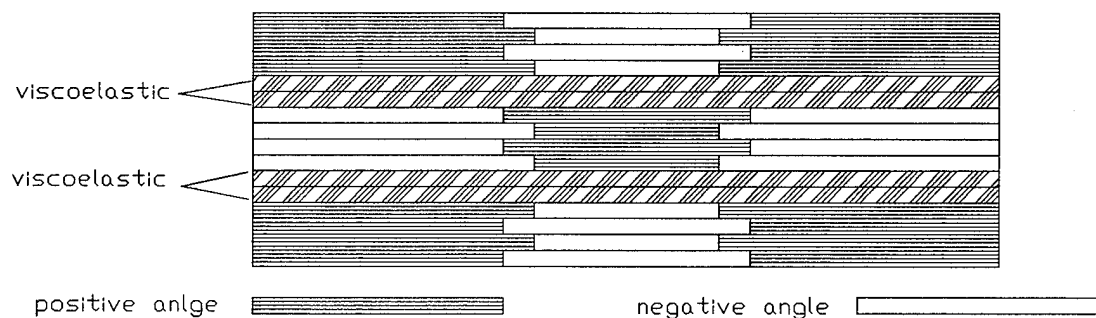
**Figure 7.**  Cross section of segmented ply construction.

endcap fibers were also oriented 18 degrees off-axis and aligned with those of the outer specimen plies.

The graphite prepreg and laminating adhesive were cut to size using straight edges, 18-degree templates, and razor blades. When all the plies were cut, they were laid up according to construction guides, similar to Figure 7, to form the different specimens.

Figure 8 shows how the specimens were placed on a small graphite epoxy tool to prevent bowing between the endcaps during the cure cycle.
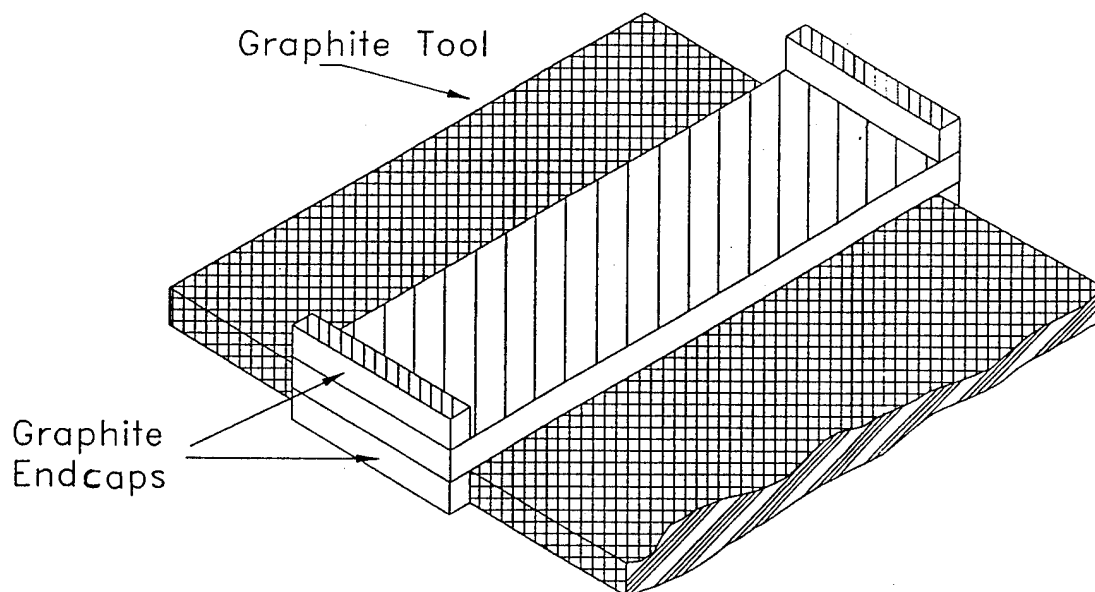


Figure 8. Graphite tooling.

The tool and specimens were sealed in standard vacuum bagging and placed in the oven. A vacuum was drawn over the specimens and they were baked for 1 hour at 250 degrees Fahrenheit per the manufacturer's instructions. After the parts cooled, they were detached from the bagging materials and the excess epoxy was removed with a belt sander.

The specimens for the second experiment were built the same way as those in the first. The dimensions and viscoelastic layer thicknesses were altered as was discussed earlier.

## Testing Validation

The testing method and apparatus were first checked by testing a specimen of known properties and then comparing the results with mathematically calculated values. A small piece of mild steel roughly equal in dimension to the composite specimens was chosen for the test. The steel sample's longitudinal frequency was calculated using the equation

$$f = \frac{1}{2L}\sqrt{\frac{E}{\mu}} \qquad (2)$$

where f is the natural frequency in hertz, E the modulus of elasticity, L the length of the sample, and $\mu$ the mass density (Blevins, 1979).

Testing consistently yielded frequency response traces

with the first fundamental peak between 17.6 and 17.8 kHz.
Table 1 lists material data and the natural frequency
calculation for the mild steel sample.

The testing procedure was further validated by building
and examining an undamped, unsegmented specimen, constructed
exactly like the other constrained layer specimens except
that no viscoelastic material was used.  This specimen
produced a fundamental peak at 19.2 kHz.  Substituting this
value and a $\mu = 1.53 \times 10^{-6}$ kg-sec$^2$/cm$^3$ into Equation 2
produces a longitudinal modulus of 51.3 Gpa or 7.44 Mpsi for
the laminate.  This value was then compared with E values
obtained from three-point bend testing and equivalent
properties calculations.  Table 2 lists the results of the
two sets of bend tests conducted.  The first set used 12-ply
unidirectional samples and the second set used samples
identical in fiber orientation to the constrained layer
damping specimens.

Table 1

Properties for Mild Steel Specimen

| Variable | Value |
| --- | --- |
| E | $2.04 \times 10^6$ kg/cm$^2$ |
| $\mu$ | $8.17 \times 10^{-6}$ kg-sec$^2$/cm$^4$ |
| L | 14cm |
| f | 17.85 kHz |

Table 2

Results of Three-Point Bend Tests

| Sample # | Width x Thickness in. | Load lb | Deflection in. |
|---|---|---|---|
| | Set #1 | | |
| 1 | 1.1 x .07 | 293 | .12 |
| 2 | 1.1 x .07 | 257 | .11 |
| 3 | 1.1 x .07 | 263 | .11 |
| 4 | 1.1 x .07 | 260 | .10 |
| 5 | 1.05 x .07 | 202 | .13 |
| 6 | 1.05 x .07 | 234 | .10 |
| | Set #2 | | |
| 1 | 1.02 x .07 | 168 | .12 |
| 2 | 1.02 x .07 | 150 | .09 |
| 3 | 1.98 x .07 | 486 | .14 |
| 4 | 1.98 x .07 | 428 | .13 |

Note. Distance between the two bottom bending points = 2 inches. Set #1 contained unidirectional specimens and set #2 contained the 18-degree off-axis research construction specimens.

The information from Table 2 was used to calculate tensile modulus values using the equation

$$E = PL^3/48yI \tag{3}$$

where E = the elastic modulus, P = the load, L = the

distance between bending supports, y = the deflection, and "I" = the moment of inertia (Higon, Ohlsew, Stiles, Weese, & Riley, 1976). Because they were of identical construction, the average tensile modulus of the second test set could be compared directly with the modulus from the impulse frequency response, but an equivalent property needed to be calculated for the unidirectional set. The equivalent property equation

$$E = 1/A_{11}' \ t \qquad\qquad (4)$$

was used for this purpose (Gibson, 1994). $A_{11}'$ is the first term of the inverted force deformation matrix and "t" stands for laminate thickness. A Classical Laminate Theory program, using the average tensile modulus from the bend tests and other material values approximated therefrom, calculated the inverted force deformation matrix (see Appendix B). Table 3 lists the modulus values and their sources.

Given the accuracy of the measuring equipment used in the three-point bend test and the natural variability of this material, these results appear adequate. The difference between the manufacturer's published tensile modulus and the calculated modulus is different because the materials used in this study were outdated, and cured in an oven without the benefits of an autoclave.

Table 3

Estimated Tensile Modulus Values

| Source | Laminate E value Gpa | $0^0$ Tensile modulus Gpa |
|---|---|---|
| Frequency Response | 51.3 | N/A |
| 3pt. Bend Identical | 64.8 | N/A |
| 3pt. Bend $0^0$ | 57.2 | 80 |
| Manufacturer's Data | N/A | 131 |

CHAPTER 4

RESULTS

Data from the first experiment were collected and analyzed using an analysis of variance statistical tool as shown in Table 4. Three loss factors were calculated and analyzed for each specimen. These three samples were left unaveraged so that information on relative efficiency would be available. Table 5 shows the raw data according to

Table 4

Analysis of Variance for Experiment #1

| Source | df | SS | MS | F | p |
|---|---|---|---|---|---|
| Block | 4 | 0.0070825 | 0.0017706 | 1.65 | >.1 |
| Design | 1 | 0.0013541 | 0.0013541 | 1.26 | >.1 |
| Width | 2 | 0.0760697 | 0.0380349 | 35.45 | <.001 |
| Design*Width | 2 | 0.0027072 | 0.0013536 | 1.25 | >.1 |
| Sample | 60 | 0.0030224 | 0.0000504 | | |
| Error | 20 | 0.0214555 | 0.0010728 | | |
| Total | 89 | 0.1116914 | | | |

Interactions combined to form error term.

| Block*Design | 4 | 0.0056663 | 0.0014166 | | |
| Block*Width | 8 | 0.0104234 | 0.0013029 | | |
| Block*Design*Width | 8 | 0.0053658 | 0.0006707 | | |
| Error | 20 | 0.0214555 | 0.0010728 | | |

Note. Alpha = .05

block and specimen type.  The analysis of variance in Table
4 shows that, of all the treatments, width was the most
important.  This is because transverse shear is generated
along the free edges of the specimen in a region
approximately equal to the laminate thickness (Jones, 1979).

Table 5

Loss Factor Data for Experiment #1

|  | 1" | | 2" | | 3" | |
|---|---|---|---|---|---|---|
|  | Seg | Con | Seg | Con | Seg | Con |
|  | 0.1099 | 0.1221 | 0.0783 | 0.0743 | 0.0364 | 0.0440 |
|  | 0.1032 | 0.1329 | 0.0838 | 0.0800 | 0.0362 | 0.0478 |
| Block #1 | 0.1023 | 0.1341 | 0.0778 | 0.0826 | 0.0326 | 0.0440 |
|  | 0.1212 | 0.1029 | 0.0901 | 0.0609 | 0.0443 | 0.0549 |
|  | 0.1291 | 0.1089 | 0.0930 | 0.0640 | 0.0406 | 0.0625 |
| Block #2 | 0.1185 | 0.1153 | 0.0959 | 0.0698 | 0.0478 | 0.0588 |
|  | 0.1155 | 0.1447 | 0.0965 | 0.1070 | 0.0370 | 0.0410 |
|  | 0.1104 | 0.1505 | 0.0963 | 0.1076 | 0.0404 | 0.0410 |
| Block #3 | 0.1118 | 0.1352 | 0.1022 | 0.1000 | 0.0332 | 0.0409 |
|  | 0.0746 | 0.0605 | 0.0811 | 0.0716 | 0.0406 | 0.0369 |
|  | 0.0751 | 0.0698 | 0.0843 | 0.0742 | 0.0369 | 0.0332 |
| Block #4 | 0.0871 | 0.0545 | 0.0816 | 0.0767 | 0.0444 | 0.0406 |
|  | 0.0947 | 0.1885 | 0.0734 | 0.0734 | 0.0255 | 0.0449 |
|  | 0.0678 | 0.1778 | 0.0760 | 0.0716 | 0.0291 | 0.0448 |
| Block #5 | 0.0997 | 0.1381 | 0.0703 | 0.0789 | 0.0291 | 0.0410 |

The narrower specimens had a greater proportion of free edge and were more dampened. The small $F$ statistics for the other treatments indicate that for the given sample size and alpha level, any observed difference in the means (listed in Table 6) likely occurred due to chance. Given the variability within designs, this experiment did not have sufficient sample size to produce significant $F$ statistics for the design treatment or the design-by-width interaction. This strongly indicates that any differences in axial

Table 6

Loss Factor Means for Experiment #1

| Block | M | Design | Width | M |
|-------|---|--------|-------|---|
| 1 | 0.079017 | Segmented | 1" | 0.10139 |
| 2 | 0.082139 | Segmented | 2" | 0.08537 |
| 3 | 0.089511 | Segmented | 3" | 0.03694 |
| 4 | 0.062428 | Constrained | 1" | 0.12239 |
| 5 | 0.079144 | Constrained | 2" | 0.07951 |
| | | Constrained | 3" | 0.04509 |
| | | Combined Means | | |
| | | Segmented | | 0.074569 |
| | | Constrained | | 0.082327 |
| | | | 1" | 0.11189 |
| | | | 2" | 0.08244 |
| | | | 3" | 0.04101 |

damping, observed between the segmented ply or constrained layer constructions, were not caused by design distinctions but were merely the product of chance variation. The trend of the overall means did, however, follow the pattern predicted by Fronk (Fronk et al., in press) as depicted in Figure 9. The axial damping in the segmented ply specimens varied with segment aspect ratio while the constrained layer specimens displayed a more linear change due to the free-edge effect.

It should be noted that the 1-inch wide specimens in
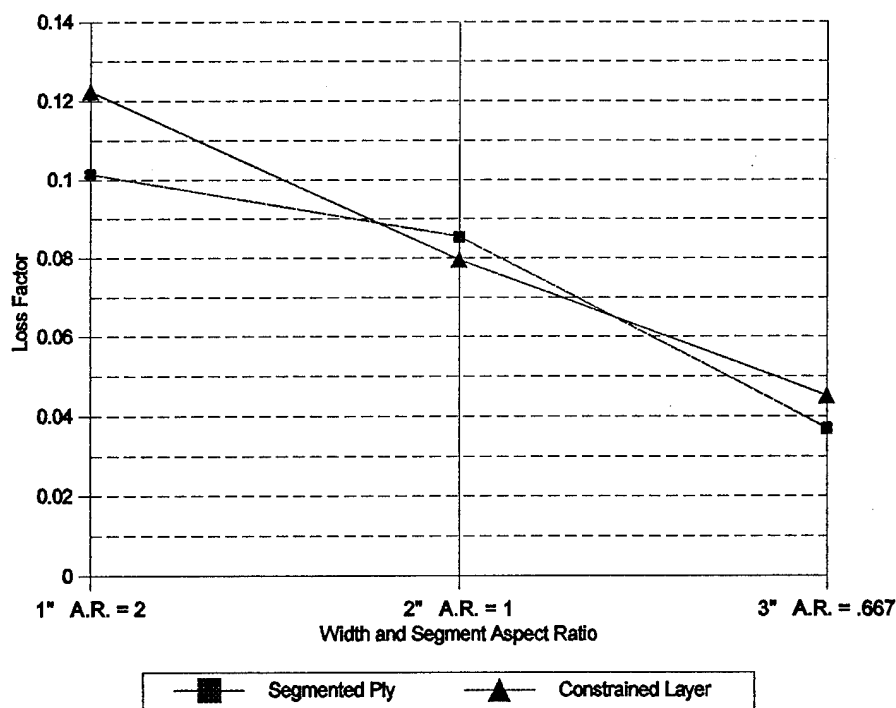


Figure 9. Plot of experiment #1 loss factor means.

the first experiment were very difficult to test consistently because of their small mass.  The data received from these samples are therefore less reliable.

The second experiment removed the width effect by studying specimens with the same external dimensions.  Three frequency response traces were recorded for each specimen as in the first experiment.  The analysis of variance statistics are shown in Table 7.  Again the sample size was not large enough, given the variance within designs, to produce a critical F statistic for the variance between designs.  The effects of segment aspect ratio were, however, much easier to see without the confounding effect of varying specimen dimensions.  It is clear from Figure 10 that the means of the segmented specimens surpassed the constrained layer mean and also that the axial damping peaked around a segment aspect ratio of one.  This correlates well with data from the first experiment and with

Table 7

Analysis of Variance for Experiment #2

| Source | df | SS | MS | F |
|--------|-----|------------|------------|-------|
| Design | 3 | 0.00027192 | 0.00009064 | 1.105 |
| Rep(Design) | 12 | 0.00098413 | 0.00008201 | |
| Sample | 32 | 0.00034255 | 0.00001070 | |
| Total | 47 | 0.00159860 | | |

earlier finite element data as well. The different segment
aspect ratios were achieved by varying the number of
segments in specimens of the same dimension. The specimens
with two segments had a segment aspect ratio of 1.5, those
with three segments had a segment aspect ratio of 1, and
those with four had a segment aspect ratio of .75.

Figure 11 shows a plot of the loss factors from each of
the 16 specimens. This shows graphically what the
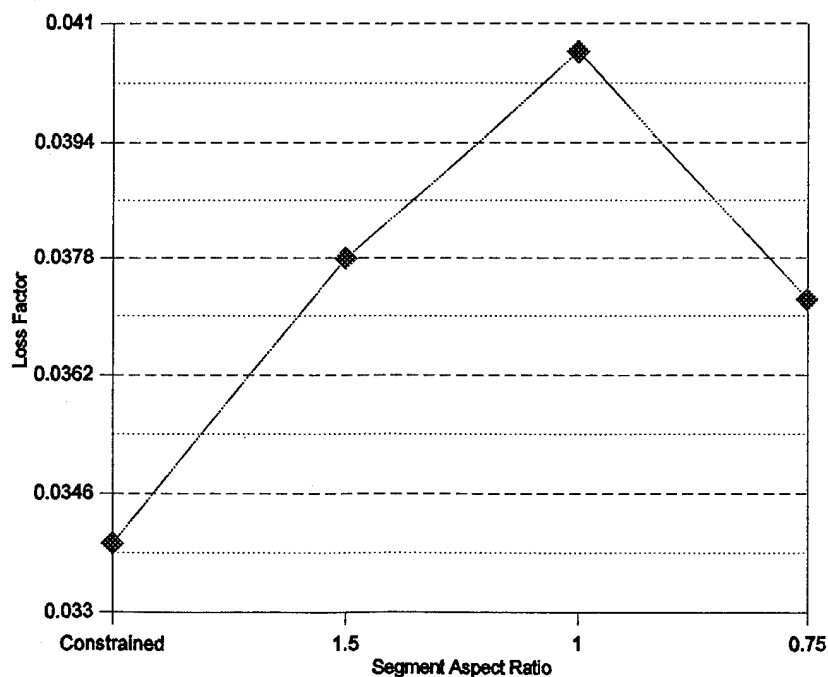


Figure 10. Plot of overall means for experiment #2.

statistical tools have already indicated; the scatter within designs is as important as the scatter between designs. In other words it could be convincingly argued that the data in Figure 11 represent a straight line and that the differences depicted in Figure 10 were the result of chance variations. Table 8 lists the means used in Figures 10 and 11.

The two-segment specimen from replication two was reexamined because it had the highest loss factor of the
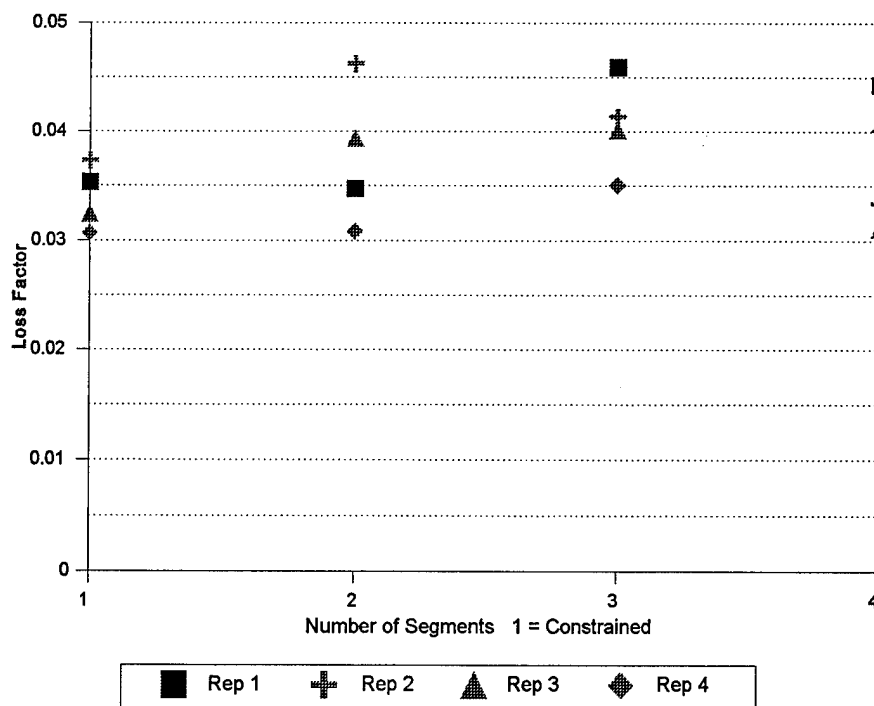


Figure 11. Scatter plot of experiment #2 means.

experiment. A small ridge running the length of the part was discovered. This ridge was caused by a small gap in the tooling plates placed under the parts during the cure cycle.

Table 8

Means for Experiment #2

| Design | Data | Design | Rep | Data |
|---|---|---|---|---|
| Constrained | 0.033925 | Constrained | 1 | 0.0360 |
| Two Segments | 0.037792 | | 2 | 0.0373 |
| Three Segments | 0.040625 | | 3 | 0.0324 |
| Four Segments | 0.037225 | | 4 | 0.0307 |
| | | Two Segments | 1 | 0.0347 |
| | | | 2 | 0.0462 |
| | | | 3 | 0.0394 |
| | | | 4 | 0.0308 |
| | | Three Segments | 1 | 0.0459 |
| | | | 2 | 0.0414 |
| | | | 3 | 0.0401 |
| | | | 4 | 0.0351 |
| | | Four Segments | 1 | 0.0443 |
| | | | 2 | 0.0334 |
| | | | 3 | 0.0311 |
| | | | 4 | 0.0401 |

CHAPTER 5

CONCLUSIONS

## Summary

The importance of the free edge in axial damping of
constrained layer fibrous composites was clearly
demonstrated in the first experiment. Unfortunately this
free-edge effect confounded the data and made
interpretations concerning segmented or unsegmented design
difficult. The small one-inch wide specimens also proved
troublesome in construction, testing, and interpretation.
In the second experiment the free-edge confounding was
avoided and less viscoelastic material was used. This
allowed the design differences to produce more pronounced
results. Still, the difference in axial damping between the
constrained layer design and the segmented ply design is
difficult to demonstrate. From a practical standpoint the
arduous nature of the segmented ply manufacture would seem
to negate any impetus for a small and unguaranteed gain in
axial damping.

## Conclusions

Constrained layer damping takes place along the free
edges of the composite in a boundary region approximately
equal in dimension to the laminate thickness (Jones, 1975).
Fronk (Fronk et al., in press) demonstrated that the

transverse shear components $\gamma_{xz}$ and $\gamma_{yz}$ account for over 99% of the strain energy in the viscoelastic layer. Almost 100% of the damping in a conventional reverse-angle constrained layer composite comes from the $\gamma_{xz}$ component, but both the $\gamma_{xz}$ and $\gamma_{yz}$ components are important in the segmented design. The increase in the $\gamma_{yz}$ comes at the expense of the $\gamma_{xz}$ but reaches a point where the combination of the two components exceeds the strain energy in the constrained layer design (Fronk et al., in press). Figure 12 depicts how the boundary regions in both designs might appear.

Composites are often favored in the development of highly damped structures because their inherent design

Segmented Ply Construction

Constrained Layer Construction
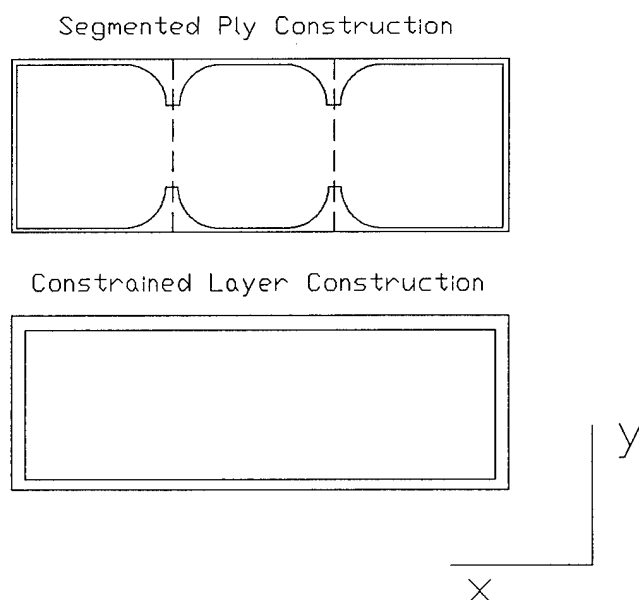
Figure 12. Boundary regions of both designs.

flexibility allows for trade-offs between stiffness and damping (Gibson, 1994). In segmented ply construction, stiffness is added over the lap joint region and reduced between the joints. It does appear that this complex arrangement could offer a minor increase in axial damping, but using more conventional methods to reduce overall stiffness would seem more practical. From a manufacturing standpoint the segmented ply design is very labor intensive and complex, which increases the problem of cost and repeatability. It is, however, conceivable that different configurations of this same design could produce more impressive results. There are perhaps, also, unique applications that might benefit from the segmented ply construction.

## Suggestions for Future Research

A more comprehensive finite element study would be the first step in better understanding the mechanisms responsible for axial damping in these designs. A wealth of other knowledge about strength, stiffness, and boundary regions could also be garnered from such a study. The completion of a closed form mathematical solution for constrained layer damping would, of course, also be invaluable. These studies should be followed by other carefully designed experimental studies, such as this one, to include the capricious nature of composite manufacture in

the equation.

Specific areas, within this design, that need to be investigated for their effect on axial damping include: maximizing the difference between the properties of the viscoelastic material and the constraining layer material, varying the fiber angle, and applying the design to different boundary conditions such as the fixed-fixed state.

After increased axial damping was observed in a slightly deformed test specimen from this study, a new specimen was built and purposefully deformed by placing a small section of copper tubing beneath it during the cure cycle. These deformations drastically changed the specimen's natural frequency and axial loss factor. This one fact alone indicates that geometry variations, more easily achieved than segmenting the lamina, should be investigated for their effects on stiffness and damping.

# REFERENCES

Blevins, R. D. (1979). Formulas for natural frequency and mode shape. New York: Van Nostrand Reinhold Co.

Dolgin, B. P. (1990). Composite damping struts for large precision structures; Patent application (1.71:NPO-17914-1-CU, 1-15). Pasadena, CA: Jet Propulsion Laboratory.

Drake, M. L. (1985, December). Passive damping: Has its time finally come? Mechanical Engineering, 107, 20-24.

Fronk, T. H., Womack, K. C., Ellis, K. D., & Finlinson, L. W. (in press). Finite element modeling of damping in constrained layer composite structures induced by inplane loads using ADINA. Computer Structures.

Gibson, R. F. (1994). Principles of composite material mechanics. New York: McGraw Hill.

Higdon, A., Ohlsew, E. H., Stiles, W. B., Weese, J. A., & Riley, W. F. (1976). Mechanics of materials. New York: John Wiley & Sons, Inc.

Jones, R. M. (1975). Mechanics of composite materials. New York: Hemisphere Publishing Corporation.

Olcott, D. D. (1992). Improved damping in composite structures through stress coupling, co-cured damping layers, and segmented stiffness layers. (Doctoral dissertation, Brigham Young University, 1992). Dissertation Abstracts International, 53, 1944B.

Saravanos, D. A., & Chamis, C. C. (1989). Unified micromechanics of damping for unidirectional and off-axis fiber composites. NASA Technical Briefs, NAS 1.15:102107: 1-25.

Suarez, S. A., & Gibson, R.F. (1986). The influence of fiber orientation on damping and stiffness of polymer composite materials. Experimental Mechanics, 26, 175-184.

Suarez, S.A., Gibson, R. F., Sun, C. T., & Debold, L. R. (1984). Random and impulse techniques for measurement of damping in composite materials. Experimental Techniques, 6, 19-24.

Sun, C. T., Gibson, R. F., & Chaturvedi, S. K. (1985).
    Internal damping of polymer matrix composites under
    off-axis loading. <u>Journal of Material Science, 20</u>,
    2575-2585.

APPENDICES

APPENDIX A.   DATA LOGS

## Data Log for 3" Segmented Specimens

Specimen Type: 3" Seg          Batch # 1

| Trace | dB-3 | $\omega_0$ | $\omega_1$ | $\omega_2$ | $\eta$ |
|-------|-------|-------|-------|-----|--------|
| 330 | 38.42 | 13.75 | 13.5 | 14 | 0.0364 |
| 331 | 37.64 | 13.8 | 13.5 | 14 | 0.0362 |
| 332 | 40.87 | 13.8 | 13.55 | 14 | 0.0326 |

Specimen Type: 3" Seg          Batch # 2

| Trace | dB-3 | $\omega_0$ | $\omega_1$ | $\omega_2$ | $\eta$ |
|-------|-------|-------|-------|-------|--------|
| 336 | 39.2 | 13.55 | 13.3 | 13.9 | 0.0443 |
| 337 | 40.61 | 13.55 | 13.3 | 13.85 | 0.0406 |
| 338 | 37.56 | 13.6 | 13.25 | 13.9 | 0.0478 |

Specimen Type: 3" Seg          Batch # 3

| Trace | dB-3 | $\omega_0$ | $\omega_1$ | $\omega_2$ | $\eta$ |
|-------|-------|-------|-------|-------|--------|
| 342 | 40.89 | 13.5 | 13.3 | 13.8 | 0.037 |
| 343 | 42.46 | 13.6 | 13.35 | 13.9 | 0.0404 |
| 344 | 44.66 | 13.55 | 13.35 | 13.8 | 0.0332 |

Specimen Type:    3" Seg          Batch #   4

| Trace | dB-3 | $\omega_0$ | $\omega_1$ | $\omega_2$ | $\eta$ |
|-------|-------|-------|-------|-------|--------|
| 348 | 44.12 | 13.55 | 13.25 | 13.8 | 0.0406 |
| 349 | 40.17 | 13.55 | 13.33 | 13.8 | 0.0369 |
| 350 | 41.17 | 13.5 | 13.2 | 13.8 | 0.0444 |

Specimen Type:    3" Seg          Batch #   5

| Trace | dB-3 | $\omega_0$ | $\omega_1$ | $\omega_2$ | $\eta$ |
|-------|-------|-------|-------|-------|--------|
| 354 | 40.93 | 13.75 | 13.6 | 13.95 | 0.0255 |
| 355 | 44.63 | 13.75 | 13.55 | 13.95 | 0.0291 |
| 356 | 41.25 | 13.75 | 13.55 | 13.95 | 0.0291 |

# Data Log for 3" Constrained Specimens

Specimen Type:   3" Con                                    Batch #    1

| Trace | dB-3 | $\omega_0$ | $\omega_1$ | $\omega_2$ | $\eta$ |
|-------|-------|-------|-------|-------|-------|
| 333 | 35.26 | 13.65 | 13.3 | 13.9 | 0.044 |
| 334 | 35.86 | 13.6 | 13.3 | 13.95 | 0.0478 |
| 335 | 38.63 | 13.65 | 13.35 | 13.95 | 0.044 |

Specimen Type:   3" Con                                    Batch #    2

| Trace | dB-3 | $\omega_0$ | $\omega_1$ | $\omega_2$ | $\eta$ |
|-------|-------|-------|-------|-------|-------|
| 339 | 38.67 | 13.65 | 13.25 | 14 | 0.0549 |
| 340 | 38.27 | 13.6 | 13.15 | 14 | 0.0625 |
| 341 | 38.9 | 13.6 | 13.2 | 14 | 0.0588 |

Specimen Type:   3" Con                                    Batch #    3

| Trace | dB-3 | $\omega_0$ | $\omega_1$ | $\omega_2$ | $\eta$ |
|-------|-------|-------|-------|-------|-------|
| 347 | 43.77 | 13.4 | 13.15 | 13.7 | 0.041 |
| 346 | 39.56 | 13.4 | 13.15 | 13.7 | 0.041 |
| 345 | 40.81 | 13.45 | 13.15 | 13.7 | 0.0409 |

Specimen Type:   3" Con                                    Batch #    4

| Trace | dB-3 | $\omega_0$ | $\omega_1$ | $\omega_2$ | $\eta$ |
|-------|-------|-------|-------|-------|-------|
| 351 | 41.54 | 13.55 | 13.3 | 13.8 | 0.0369 |
| 352 | 42.82 | 13.55 | 13.3 | 13.75 | 0.0332 |
| 353 | 37.58 | 13.55 | 13.25 | 13.8 | 0.0406 |

Specimen Type:   3" Con                                    Batch #    5

| Trace | dB-3 | $\omega_0$ | $\omega_1$ | $\omega_2$ | $\eta$ |
|-------|-------|-------|-------|-------|-------|
| 357 | 39.57 | 13.35 | 13.05 | 13.65 | 0.0449 |
| 358 | 40.88 | 13.4 | 13.1 | 13.7 | 0.0448 |
| 359 | 39.96 | 13.4 | 13.15 | 13.7 | 0.041 |

## Data Log for 2" Segmented Specimens

Specimen Type: 2" Seg                                    Batch #   1

| Trace | dB-3 | $\omega_0$ | $\omega_1$ | $\omega_2$ | $\eta$ |
|---|---|---|---|---|---|
| 306 | 41.23 | 17.25 | 16.7 | 18.05 | 0.0783 |
| 307 | 41 | 17.3 | 16.7 | 18.15 | 0.0838 |
| 308 | 43.4 | 17.35 | 16.7 | 18.05 | 0.0778 |

Specimen Type: 2" Seg                                    Batch #   2

| Trace | dB-3 | $\omega_0$ | $\omega_1$ | $\omega_2$ | $\eta$ |
|---|---|---|---|---|---|
| 312 | 40.91 | 17.2 | 16.5 | 18.05 | 0.0901 |
| 313 | 39.75 | 17.2 | 16.6 | 18.2 | 0.093 |
| 314 | 38.93 | 17.2 | 16.6 | 18.25 | 0.0959 |

Specimen Type: 2" Seg                                    Batch #   3

| Trace | dB-3 | $\omega_0$ | $\omega_1$ | $\omega_2$ | $\eta$ |
|---|---|---|---|---|---|
| 300 | 35.88 | 16.05 | 15.2 | 16.75 | 0.0965 |
| 301 | 36.04 | 16.1 | 15.35 | 16.9 | 0.0963 |
| 302 | 35.36 | 16.15 | 15.25 | 16.9 | 0.1022 |

Specimen Type: 2" Seg                                    Batch #   4

| Trace | dB-3 | $\omega_0$ | $\omega_1$ | $\omega_2$ | $\eta$ |
|---|---|---|---|---|---|
| 318 | 40.21 | 16.65 | 16.05 | 17.4 | 0.0811 |
| 319 | 41.1 | 16.6 | 15.85 | 17.25 | 0.0843 |
| 320 | 40.84 | 16.55 | 15.9 | 17.25 | 0.0816 |

Specimen Type: 2" Seg                                    Batch #   5

| Trace | dB-3 | $\omega_0$ | $\omega_1$ | $\omega_2$ | $\eta$ |
|---|---|---|---|---|---|
| 324 | 42.18 | 16.35 | 15.8 | 17 | 0.0734 |
| 325 | 42.4 | 16.45 | 15.85 | 17.1 | 0.076 |
| 326 | 40.44 | 16.35 | 15.85 | 17 | 0.0703 |

## Data Log for 2" Constrained Specimens

Specimen Type: 2" Con                                    Batch #   1

| Trace | dB-3 | $\omega_0$ | $\omega_1$ | $\omega_2$ | $\eta$ |
|-------|------|------------|------------|------------|--------|
| 309 | 42.73 | 17.5 | 17 | 18.3 | 0.0743 |
| 310 | 42.59 | 17.5 | 16.8 | 18.2 | 0.08 |
| 311 | 42.03 | 17.55 | 16.8 | 18.25 | 0.0826 |

Specimen Type: 2" Con                                    Batch #   2

| Trace | dB-3 | $\omega_0$ | $\omega_1$ | $\omega_2$ | $\eta$ |
|-------|------|------------|------------|------------|--------|
| 315 | 43.74 | 17.25 | 16.8 | 17.8 | 0.0609 |
| 316 | 42.54 | 17.2 | 16.75 | 17.85 | 0.064 |
| 317 | 43.83 | 17.2 | 16.6 | 17.8 | 0.0698 |

Specimen Type: 2" Con                                    Batch #   3

| Trace | dB-3 | $\omega_0$ | $\omega_1$ | $\omega_2$ | $\eta$ |
|-------|------|------------|------------|------------|--------|
| 303 | 39.94 | 16.35 | 15.65 | 17.4 | 0.107 |
| 304 | 37.77 | 15.8 | 14.8 | 16.5 | 0.1076 |
| 305 | 40.25 | 16.5 | 15.55 | 17.2 | 0.1 |

Specimen Type: 2" Con                                    Batch #   4

| Trace | dB-3 | $\omega_0$ | $\omega_1$ | $\omega_2$ | $\eta$ |
|-------|------|------------|------------|------------|--------|
| 321 | 42.35 | 16.75 | 16.1 | 17.3 | 0.0716 |
| 322 | 42.52 | 16.85 | 16.15 | 17.4 | 0.0742 |
| 323 | 41.56 | 16.95 | 16.25 | 17.55 | 0.0767 |

Specimen Type: 2" Con                                    Batch #   5

| Trace | dB-3 | $\omega_0$ | $\omega_1$ | $\omega_2$ | $\eta$ |
|-------|------|------------|------------|------------|--------|
| 327 | 40.5 | 16.7 | 16.15 | 17.375 | 0.0734 |
| 328 | 39.32 | 16.75 | 16.15 | 17.375 | 0.0716 |
| 329 | 39.87 | 17.1 | 16.05 | 17.4 | 0.0789 |

## Data Log for 1" Segmented Specimens

Specimen Type: 1" Seg                                    Batch #   1

| Trace | dB-3 | $\omega_0$ | $\omega_1$ | $\omega_2$ | $\eta$ |
|-------|------|------------|------------|------------|--------|
| 360   | 42.35 | 17.75 | 16.95 | 18.9  | 0.1099 |
| 361   | 41.8  | 17.45 | 16.4  | 18.2  | 0.1032 |
| 362   | 42.4  | 17.6  | 16.85 | 18.65 | 0.1023 |

Specimen Type: 1" Seg                                    Batch #   2

| Trace | dB-3 | $\omega_0$ | $\omega_1$ | $\omega_2$ | $\eta$ |
|-------|------|------------|------------|------------|--------|
| 366   | 39.57 | 16.5  | 15.55 | 17.55 | 0.1212 |
| 367   | 41.64 | 16.65 | 15.8  | 17.95 | 0.1291 |
| 368   | 42.93 | 16.45 | 15.74 | 17.6  | 0.1185 |

Specimen Type: 1" Seg                                    Batch #   3

| Trace | dB-3 | $\omega_0$ | $\omega_1$ | $\omega_2$ | $\eta$ |
|-------|------|------------|------------|------------|--------|
| 372   | 41.52 | 16.45 | 15.35 | 17.25 | 0.1155 |
| 373   | 40.43 | 16.3  | 15.35 | 17.15 | 0.1104 |
| N/A   | 38.7  | 16.55 | 15.35 | 17.2  | 0.1118 |

Specimen Type: 1" Seg                                    Batch #   4

| Trace | dB-3 | $\omega_0$ | $\omega_1$ | $\omega_2$ | $\eta$ |
|-------|------|------------|------------|------------|--------|
| 378   | 44.25 | 16.75 | 16.05 | 17.3  | 0.0746 |
| 379   | 44.28 | 16.65 | 16.15 | 17.4  | 0.0751 |
| 380   | 43.36 | 16.65 | 16.15 | 17.6  | 0.0871 |

Specimen Type: 1" Seg                                    Batch #   5

| Trace | dB-3 | $\omega_0$ | $\omega_1$ | $\omega_2$ | $\eta$ |
|-------|------|------------|------------|------------|--------|
| 384   | 43.64 | 16.9  | 16.3  | 17.9  | 0.0947 |
| 385   | 45.9  | 16.95 | 16.5  | 17.65 | 0.0678 |
| 386   | 44.49 | 17.05 | 16.3  | 18    | 0.0997 |

## Data Log for 1" Constrained Specimens

Specimen Type: 1" Con                                    Batch #    1

| Trace | dB-3 | $\omega_0$ | $\omega_1$ | $\omega_2$ | $\eta$ |
|-------|------|------------|------------|------------|--------|
| 363   | 41.5 | 17.2       | 16.4       | 18.5       | .1221  |
| 364   | 42.38 | 17.3      | 16.4       | 18.7       | .1329  |
| 365   | 40.06 | 17.15     | 16.1       | 18.4       | .1341  |

Specimen Type: 1" Con                                    Batch #    2

| Trace | dB-3 | $\omega_0$ | $\omega_1$ | $\omega_2$ | $\eta$ |
|-------|------|------------|------------|------------|--------|
| 369   | 42.21 | 17.5      | 16.5       | 18.3       | .1029  |
| 370   | 41.95 | 17.45     | 16.4       | 18.3       | .1089  |
| 371   | 43    | 17.35     | 16.25      | 18.25      | .1153  |

Specimen Type: 1" Con                                    Batch #    3

| Trace | dB-3 | $\omega_0$ | $\omega_1$ | $\omega_2$ | $\eta$ |
|-------|------|------------|------------|------------|--------|
| 375   | 40.30 | 15.9      | 15.05      | 17.35      | .1447  |
| 376   | 41.66 | 15.95     | 14.9       | 17.3       | .1505  |
| 377   | 40.44 | 15.9      | 14.85      | 17.1       | .1352  |

Specimen Type: 1" Con                                    Batch #    4

| Trace | dB-3 | $\omega_0$ | $\omega_1$ | $\omega_2$ | $\eta$ |
|-------|------|------------|------------|------------|--------|
| 381   | 46.15 | 15.7      | 15.15      | 16.1       | .0605  |
| 382   | 46.89 | 15.75     | 15.2       | 16.3       | .0698  |
| 383   | 45.83 | 15.6      | 15.2       | 16.05      | .0545  |

Specimen Type: 1" Con                                    Batch # 5

| Trace | dB-3 | $\omega_0$ | $\omega_1$ | $\omega_2$ | $\eta$ |
|-------|------|------------|------------|------------|--------|
| 387   | 39.28 | 15.65     | 14.1       | 17.05      | .1885  |
| 388   | 40.28 | 15.75     | 14.2       | 17         | .1778  |
| 389   | 36.70 | 16.65     | 15.25      | 17.55      | .1381  |

## Data Log for No-Segment 9" x 3" Specimens

Specimen Type: No Segment                    Batch #    9" x 3"

| Trace | dB-3 | $\omega_0$ | $\omega_1$ | $\omega_2$ | $\eta$ |
|-------|------|------------|------------|------------|--------|
| 200 | 41.09 | 12.675 | 12.5 | 12.975 | .0375 |
| 201 | 42.73 | 12.775 | 12.5 | 12.95 | .0352 |
| 202 | 42.73 | 12.775 | 12.5 | 12.95 | .0352 |

Specimen Type: No Segment                    Batch #    9" x 3"

| Trace | dB-3 | $\omega_0$ | $\omega_1$ | $\omega_2$ | $\eta$ |
|-------|------|------------|------------|------------|--------|
| 215 | 38.56 | 13.00 | 12.725 | 13.175 | .0346 |
| 216 | 38.17 | 12.925 | 12.7 | 13.20 | .0387 |
| 217 | 38.00 | 12.95 | 12.675 | 13.175 | .0386 |

Specimen Type: No Segment                    Batch #    9" x 3"

| Trace | dB-3 | $\omega_0$ | $\omega_1$ | $\omega_2$ | $\eta$ |
|-------|------|------------|------------|------------|--------|
| 221 | 43.98 | 12.6 | 12.375 | 12.725 | .0278 |
| 222 | 40.33 | 12.575 | 12.375 | 12.775 | .0318 |
| 223 | 41.33 | 12.625 | 12.375 | 12.85 | .0376 |

Specimen Type: No Segment                    Batch #    9" x 3"

| Trace | dB-3 | $\omega_0$ | $\omega_1$ | $\omega_2$ | $\eta$ |
|-------|------|------------|------------|------------|--------|
| 227 | 36.19 | 12.975 | 12.825 | 13.250 | .0328 |
| 228 | 34.35 | 13.1 | 12.85 | 13.275 | .0324 |
| 300 | 35.54 | 13.05 | 12.875 | 13.225 | .0268 |

## Data Log for Two-Segment 9" x 3" Specimens

Specimen Type: Two Segments  Batch #   9" x 3"

| Trace | dB-3 | $\omega_0$ | $\omega_1$ | $\omega_2$ | $\eta$ |
|-------|------|------------|------------|------------|--------|
| 206 | 41.95 | 12.5 | 12.275 | 12.675 | .0320 |
| 207 | 41.61 | 12.45 | 12.25 | 12.65 | .0321 |
| 208 | 41.70 | 12.475 | 12.2 | 12.7 | .0401 |

Specimen Type: Two Segments  Batch #   9" x 3"

| Trace | dB-3 | $\omega_0$ | $\omega_1$ | $\omega_2$ | $\eta$ |
|-------|------|------------|------------|------------|--------|
| 209 | 43.53 | 12.375 | 12.150 | 12.675 | .0424 |
| 210 | 41.94 | 12.425 | 12.150 | 12.70 | .0443 |
| 211 | 41.49 | 12.5 | 12.05 | 12.7 | .0520 |

Specimen Type: Two Segments  Batch #   9" x 3"

| Trace | dB-3 | $\omega_0$ | $\omega_1$ | $\omega_2$ | $\eta$ |
|-------|------|------------|------------|------------|--------|
| 224 | 41.5 | 12.325 | 12.050 | 12.575 | .0426 |
| 225 | 41.34 | 12.30 | 12.075 | 12.525 | .0366 |
| 226 | 40.61 | 12.20 | 12.075 | 12.550 | .0389 |

Specimen Type: Two Segments  Batch #   9" x 3"

| Trace | dB-3 | $\omega_0$ | $\omega_1$ | $\omega_2$ | $\eta$ |
|-------|------|------------|------------|------------|--------|
| 304 | 40.35 | 12.450 | 12.30 | 12.650 | .0281 |
| 305 | 40.81 | 12.425 | 12.225 | 12.650 | .0342 |
| 306 | 41.22 | 12.425 | 12.275 | 12.650 | .0302 |

## Data Log for Three-segment 9" x 3" Specimens

Specimen Type: Three Segments          Batch #    9" x 3"

| Trace | dB-3 | $\omega_0$ | $\omega_1$ | $\omega_2$ | $\eta$ |
|-------|-------|-------|-------|-------|-------|
| 203 | 39.07 | 12.525 | 12.350 | 12.90 | .0439 |
| 204 | 41.19 | 12.55 | 12.325 | 12.90 | .0458 |
| 205 | 40.39 | 12.50 | 12.30 | 12.90 | .0480 |

Specimen Type: Three Segments          Batch #    9" x 3"

| Trace | dB-3 | $\omega_0$ | $\omega_1$ | $\omega_2$ | $\eta$ |
|-------|-------|-------|-------|-------|-------|
| 212 | 39.79 | 12.50 | 12.25 | 12.75 | .0400 |
| 213 | 43.29 | 12.5 | 12.25 | 12.775 | .0420 |
| 214 | 43.04 | 12.475 | 12.225 | 12.75 | .0421 |

Specimen Type: Three Segments          Batch #    9" x 3"

| Trace | dB-3 | $\omega_0$ | $\omega_1$ | $\omega_2$ | $\eta$ |
|-------|-------|-------|-------|-------|-------|
| 218 | 39.94 | 12.675 | 12.425 | 12.925 | .0394 |
| 219 | 38.81 | 12.650 | 12.425 | 12.95 | .0415 |
| 220 | 41.04 | 12.650 | 12.475 | 12.975 | .0395 |

Specimen Type: Three Segments          Batch #    9" x 3"

| Trace | dB-3 | $\omega_0$ | $\omega_1$ | $\omega_2$ | $\eta$ |
|-------|-------|-------|-------|-------|-------|
| 301 | 36.14 | 12.60 | 12.350 | 12.850 | .0397 |
| 302 | 38.75 | 12.60 | 12.425 | 12.80 | .0298 |
| 303 | 37.41 | 12.575 | 12.425 | 12.875 | .0358 |

## Data Log for Four-Segment 9" x 3" Specimens

Specimen Type: Four Segments          Batch #    9" x 3"

| Trace | dB-3 | $\omega_0$ | $\omega_1$ | $\omega_2$ | $\eta$ |
|-------|------|------------|------------|------------|--------|
| 307 | 40.13 | 12.6 | 12.35 | 12.875 | .0417 |
| 308 | 46.64 | 12.65 | 12.275 | 12.875 | .0475 |
| 309 | 44.26 | 12.575 | 12.275 | 12.825 | .0437 |

Specimen Type: Four Segments          Batch #    9" x 3"

| Trace | dB-3 | $\omega_0$ | $\omega_1$ | $\omega_2$ | $\eta$ |
|-------|------|------------|------------|------------|--------|
| 310 | 36.57 | 12.950 | 12.825 | 12.225 | .0309 |
| 311 | 36.83 | 13.00 | 12.775 | 13.225 | .0346 |
| 312 | 35.63 | 12.975 | 12.800 | 13.250 | .0347 |

Specimen Type: Four Segments          Batch #    9" x 3"

| Trace | dB-3 | $\omega_0$ | $\omega_1$ | $\omega_2$ | $\eta$ |
|-------|------|------------|------------|------------|--------|
| 313 | 46.26 | 12.350 | 12.175 | 12.550 | .0304 |
| 314 | 42.26 | 12.3 | 12.125 | 12.55 | .0346 |
| 315 | 43.25 | 12.40 | 12.20 | 12.55 | .0282 |

Specimen Type: Four Segments          Batch #    9" x 3"

| Trace | dB-3 | $\omega_0$ | $\omega_1$ | $\omega_2$ | $\eta$ |
|-------|------|------------|------------|------------|--------|
| 316 | 42.88 | 12.45 | 12.10 | 12.575 | .0382 |
| 317 | 42.16 | 12.475 | 12.150 | 12.650 | .0401 |
| 318 | 44.50 | 12.450 | 12.175 | 12.70 | .0421 |

APPENDIX B.   COMPUTER OUTPUT

**Classical Laminate Theory Program Output**

```
Ply #  1      E1=80Gpa   E2=6.4Gpa   G12=4Gpa   v12=.22
 Theta =  18.00    Thickness =    .14000
 [Qbar]
        .6740726E+02            .7261685E+01            .1890666E+02
        .7261685E+01            .7632159E+01            .2807915E+01
        .1890666E+02            .2807915E+01            .9898212E+01


 [Sbar]
        .3250307E-01           -.9026162E-02           -.5952386E-01
       -.9026162E-02            .1487993E+00           -.2497027E-01
       -.5952386E-01           -.2497027E-01            .2218089E+00



Ply #  5
Theta = -18.00    Thickness =    .14000
 [Qbar]
        .6740726E+02            .7261685E+01           -.1890666E+02
        .7261685E+01            .7632159E+01           -.2807915E+01
       -.1890666E+02           -.2807915E+01            .9898212E+01


 [Sbar]
        .3250307E-01           -.9026162E-02            .5952386E-01
       -.9026162E-02            .1487993E+00            .2497027E-01
        .5952386E-01            .2497027E-01            .2218089E+00


 [A]
        .1132442E+03            .1219963E+02            .1058773E+02
        .1219963E+02            .1282203E+02            .1572432E+01
        .1058773E+02            .1572432E+01            .1662900E+02


 [B]
       -.2575717E-13           -.2886580E-14           -.1776357E-14
       -.2886580E-14           -.2664535E-14           -.2220446E-15
       -.1776357E-14           -.2220446E-15           -.3552714E-14


 [D]
        .2663503E+02            .2869353E+01            .6917317E+01
        .2869353E+01            .3015741E+01            .1027322E+01
        .6917317E+01            .1027322E+01            .3911140E+01

[A] [B]   -1
[B] [D]
 .104E-01 -.915E-02 -.573E-02  .168E-16 -.451E-17 -.295E-16
-.915E-02  .870E-01 -.240E-02 -.415E-17  .767E-16 -.142E-16
-.573E-02 -.240E-02  .640E-01 -.285E-16 -.130E-16  .109E-15
 .168E-16 -.415E-17 -.285E-16  .714E-01 -.274E-01 -.119E+00
-.451E-17  .767E-16 -.130E-16 -.274E-01  .375E+00 -.500E-01
-.295E-16 -.142E-16  .109E-15 -.119E+00 -.500E-01  .480E+00
```

Table B1

<u>Breakdown of Shear Coupling Coefficients for Fiber Angle</u>

| <u>Theta</u> | <u>Vxy</u> | <u>Nxy,x</u> | <u>Nxy,y</u> |
|---|---|---|---|
| 0. | .220000 | .000000 | .000000 |
| 1. | .220665 | .304724 | .007600 |
| 2. | .222613 | .599138 | .015228 |
| 3. | .225707 | .874026 | .022912 |
| 4. | .229746 | 1.122116 | .030678 |
| 5. | .234487 | 1.338558 | .038554 |
| 6. | .239677 | 1.520978 | .046567 |
| 7. | .245078 | 1.669199 | .054744 |
| 8. | .250479 | 1.784763 | .063110 |
| 9. | .255712 | 1.870383 | .071693 |
| 10. | .260646 | 1.929436 | .080516 |
| 11. | .265189 | 1.965555 | .089604 |
| 12. | .269280 | 1.982323 | .098982 |
| 13. | .272887 | 1.983091 | .108672 |
| 14. | .275995 | 1.970865 | .118698 |
| 15. | .278605 | 1.948267 | .129082 |
| 16. | .280726 | 1.917532 | .139844 |
| 17. | .282377 | 1.880535 | .151007 |
| 18. | .283578 | 1.838826 | .162589 |

<u>Note.</u>  Material Type=AKZO Fortafil  E1=80Gpa  E2=6.4Gpa
G12=4Gpa  v12=.22

APPENDIX C.   MANUFACTURER'S DATA

**Manufacturer's Prepreg Data**

# AKZO

Old Cardiff Road
P.O. Box 357
Rockwood, TN 37854
(615)354-4120

Technical
Data Sheet
**872D**

FORTAFIL ® 3(C) PREPREGS

Fortafil ® prepregs are available with intermediate modulus Fortafil ® 3 carbon fibers. A variety of combinations can be supplied with various resin contents, fiber areal weights, and backings. Uses include commercial, industrial, and recreational products.

---

**Resin Systems**

| | |
|---|---|
| Type | 250°F Cure Epoxy |
| Resin Designation | 8601 (other tacks available) |
| Cure Conditions | 1 hr. @ 250°F |
| Volatiles Content | <0.2% |
| Gel Time | 10-15 min. @ 250°F |
| Shelf Life @ RT | 30 days min. |
| Shelf Life @ 0° F | 12 months min. |
| Glass Transition Temp. (Tg) | 275°F |

---

**Typical Fiber Properties** (Impregnated strand test)

| | |
|---|---|
| Tensile Strength | 550 ksi |
| Tensile Modulus | 33 ksi |
| Ultimate Elogation | 1.7% |

---

**Prepreg Characteristics**

| | |
|---|---|
| Width | 12" or 24" |
| Fiber Type | Fortafil ® 3(C) |
| Fiber Areal Weight (FAW) Range Available | 120-190 g/m² |
| Resin Content Range Available | 34-42% |
| Backings Available | None.  104 or 108 glass scrim |

---

**Typical Laminate Properties -8601**
(150 FAW, 250°F epoxy, no scrim, 60 V% loading)

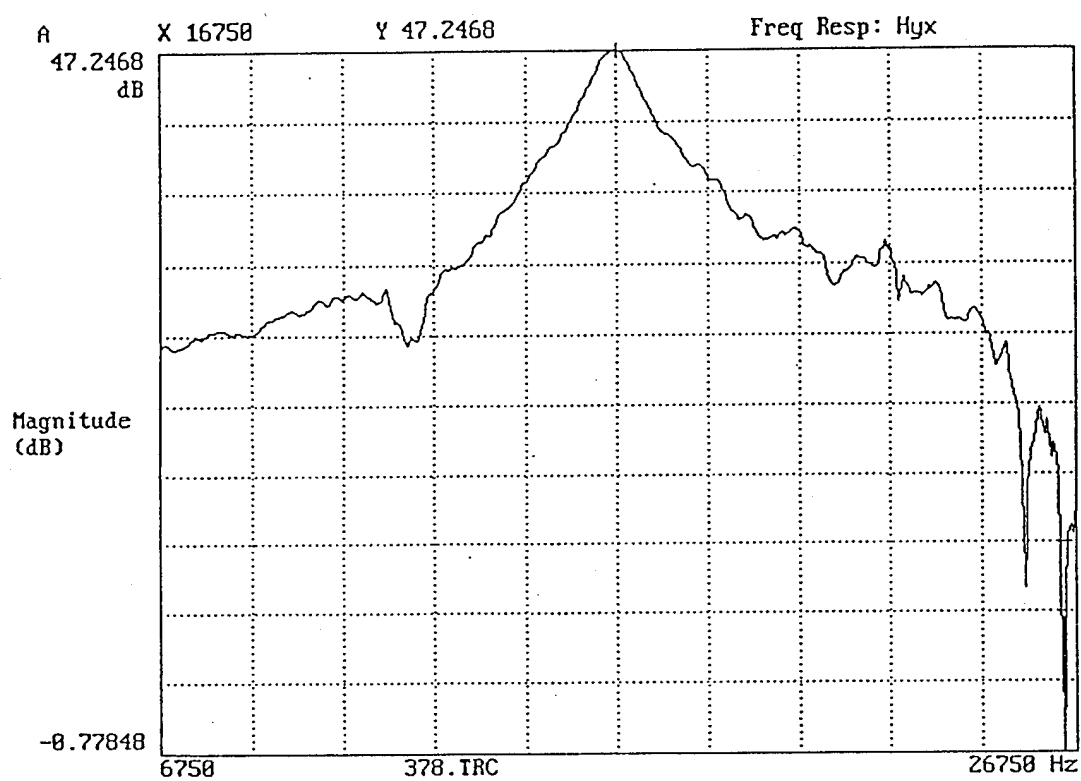| | | |
|---|---|---|
| 0° Tensile Strength | 264 ksi | 1820 Mpa |
| 0° Tensile Modulus | 19 Msi | 130 Gpa |
| 0° Flexural Strength | 300 ksi | 2070 Mpa |
| 0° Flexural Modulus | 18 Msi | 120 Gpa |
| Shear Strength (short beam) | 15 ksi | 97 Mpa |
| Cured  Ply Thickness | 5.6 x 10⁻³ in | 0.14 mm |

APPENDIX D.   FREQUENCY RESPONSE EXAMPLES

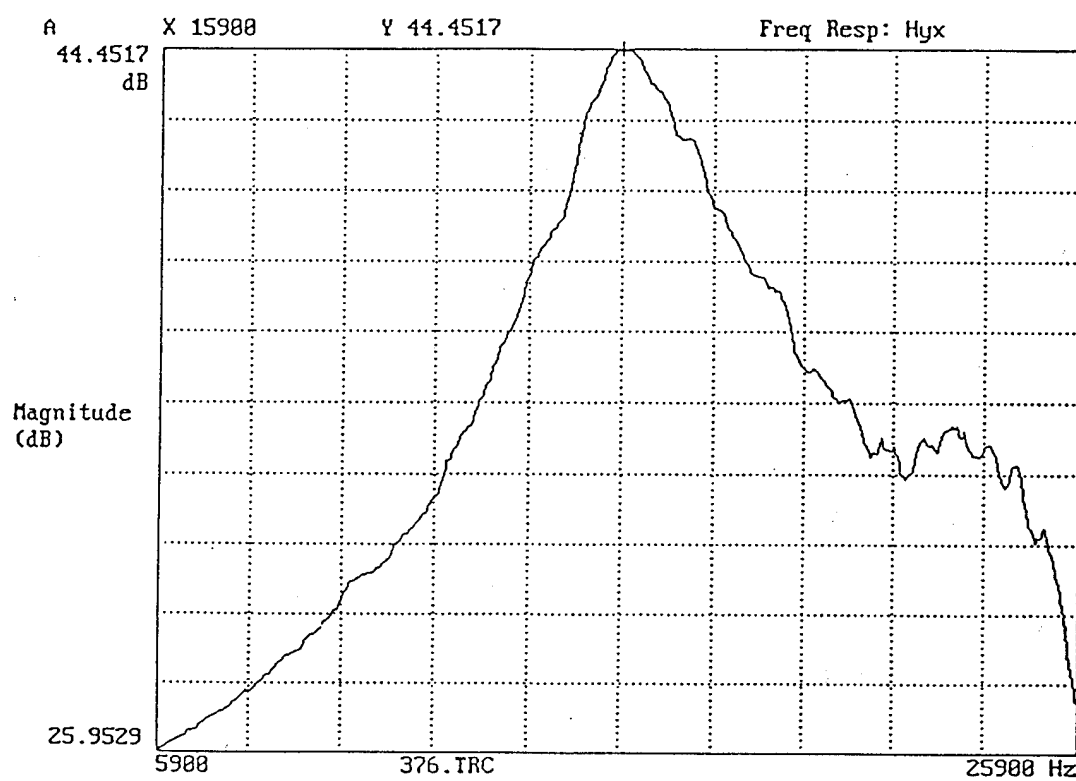Figure 13. (1" segmented example) Frequency response trace.

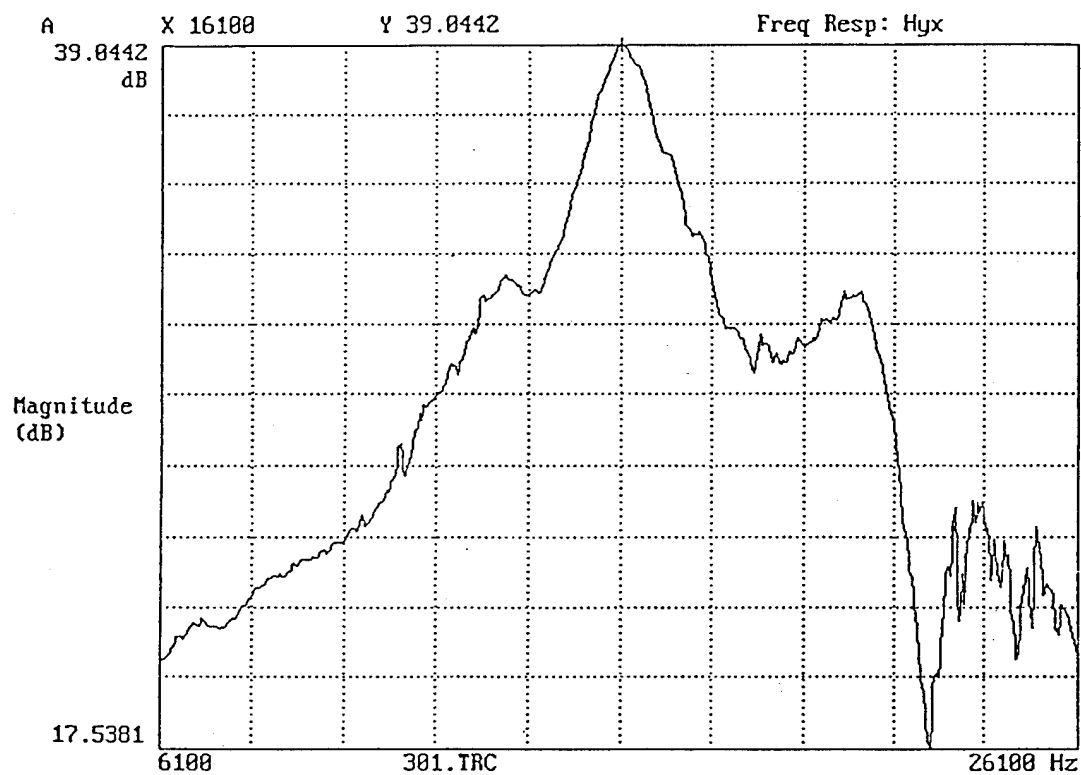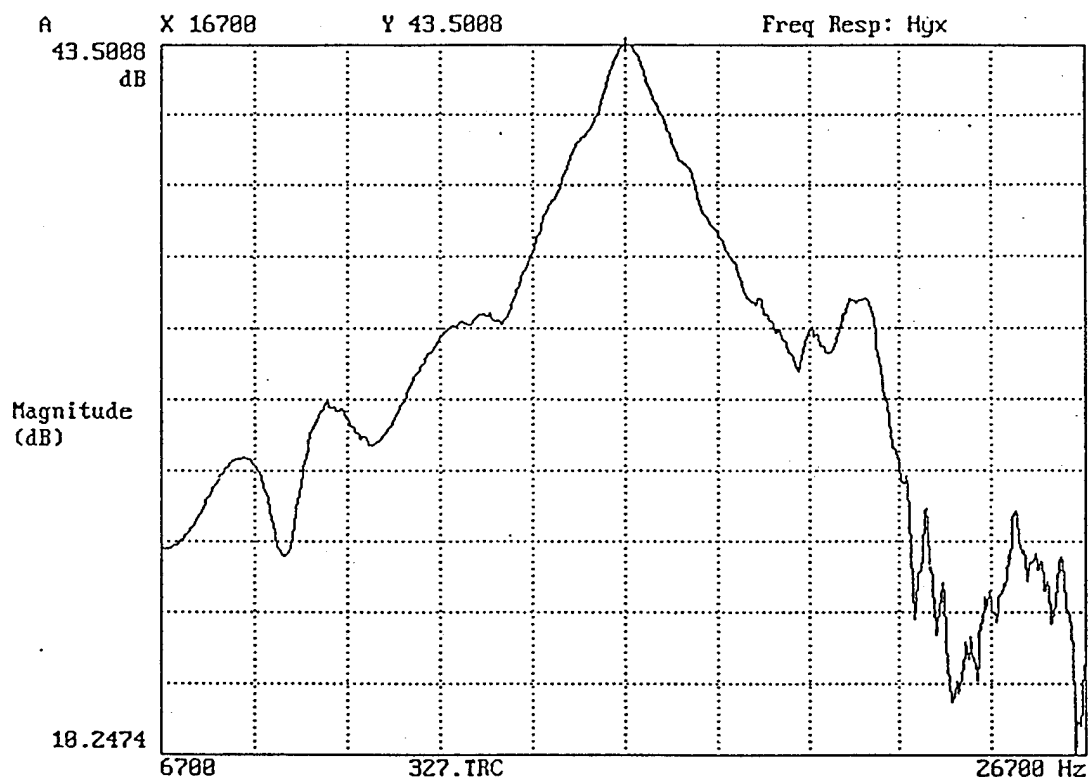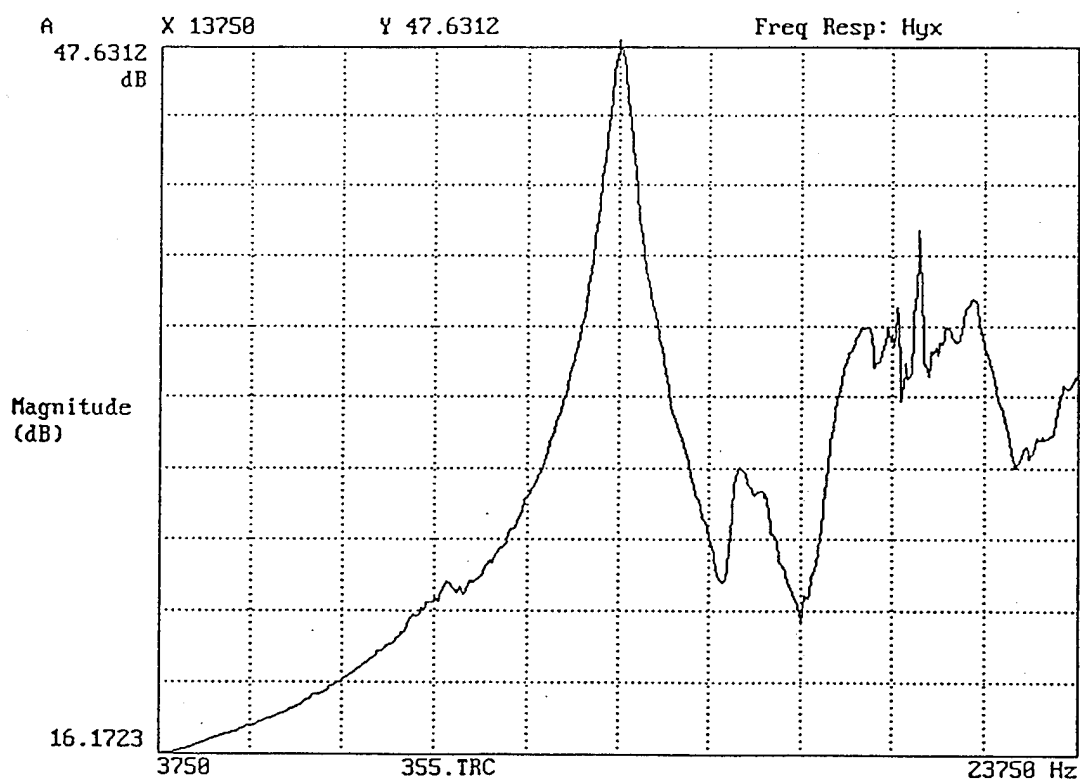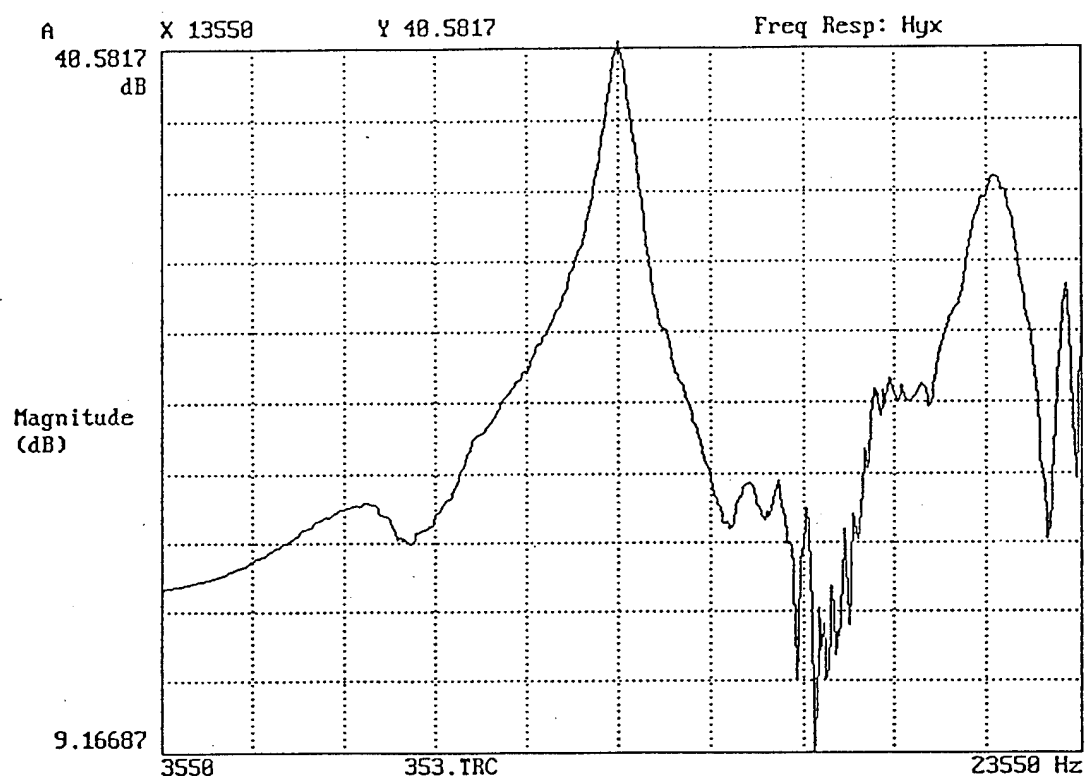Figure 14. (1" constrained example) Frequency response trace.

A    X 16100        Y 39.0442              Freq Resp: Hyx
39.0442
dB

Magnitude
(dB)

17.5381
6100              301.TRC                    26100 Hz

Figure 15.  (2" segmented example) Frequency response trace.

**Figure 16.** (2" constrained example) Frequency response trace.

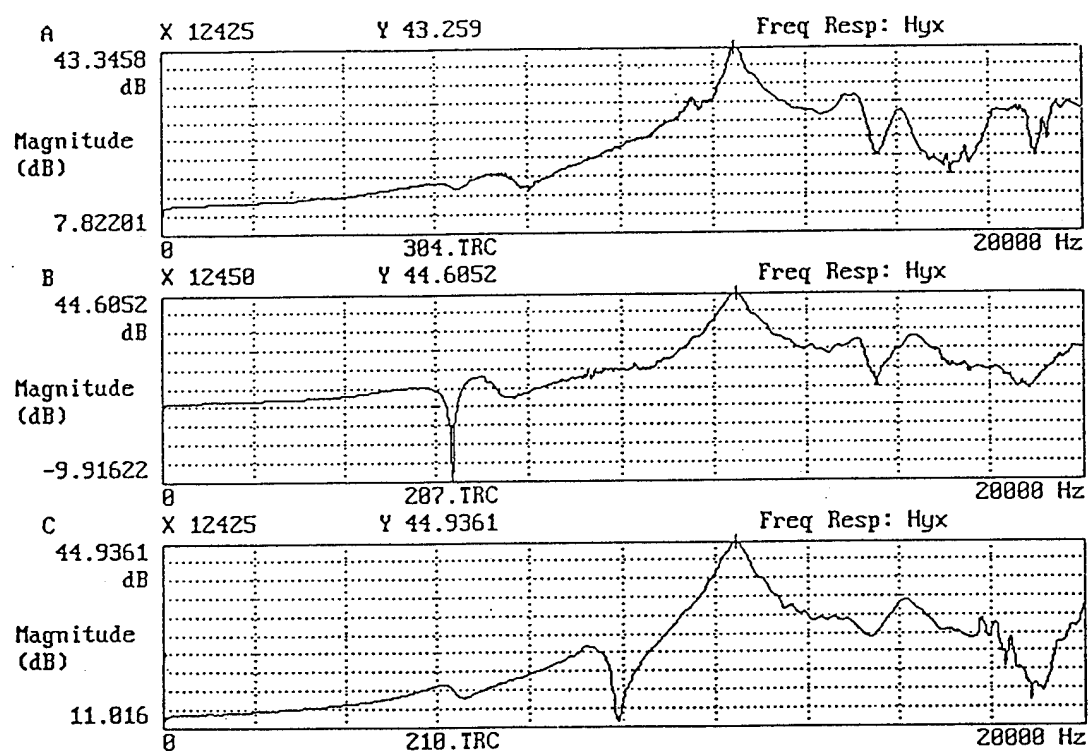Figure 17. (3" segmented example) Frequency response trace.

**Figure 18.** (3" constrained example) Frequency response trace.
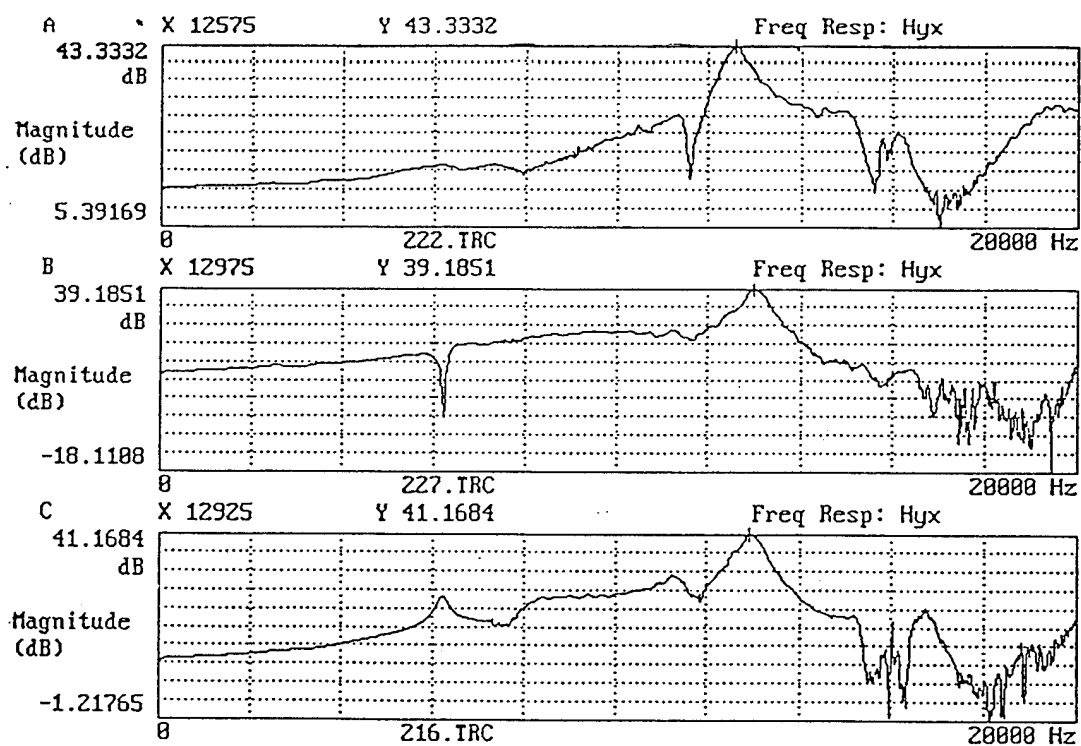
Figure 19. (No-segment example) Frequency response trace for 9" x 3" specimen.

Figure 20.  (Two-segment example) Frequency response trace
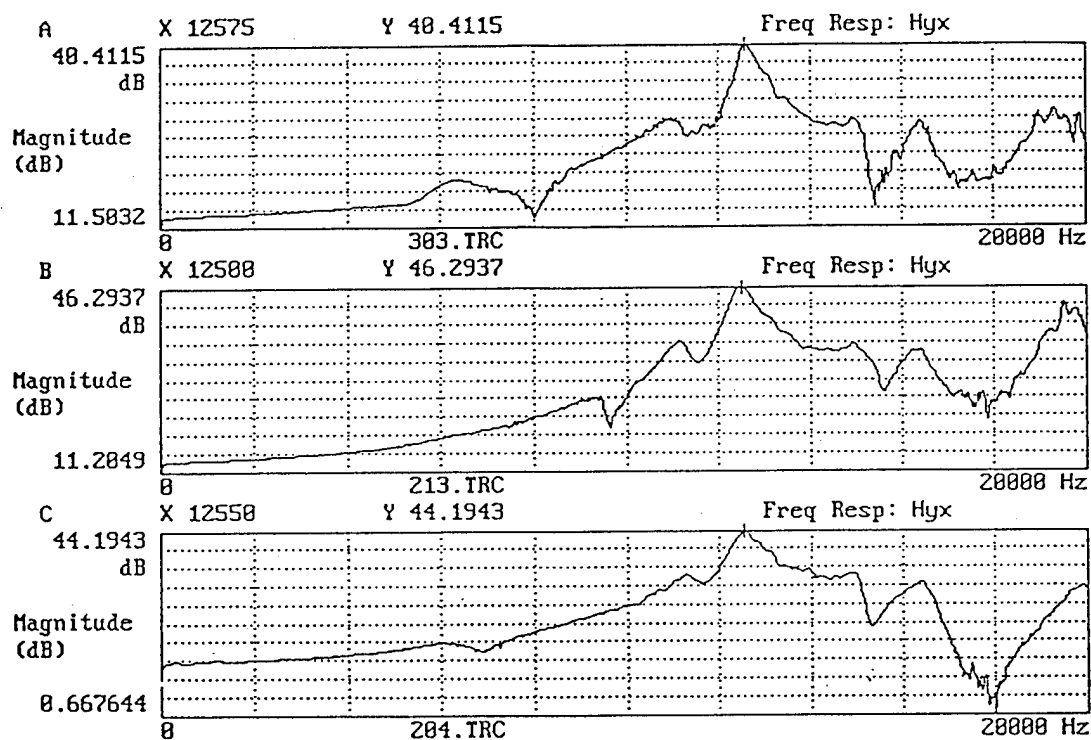for 9" x 3" specimen.

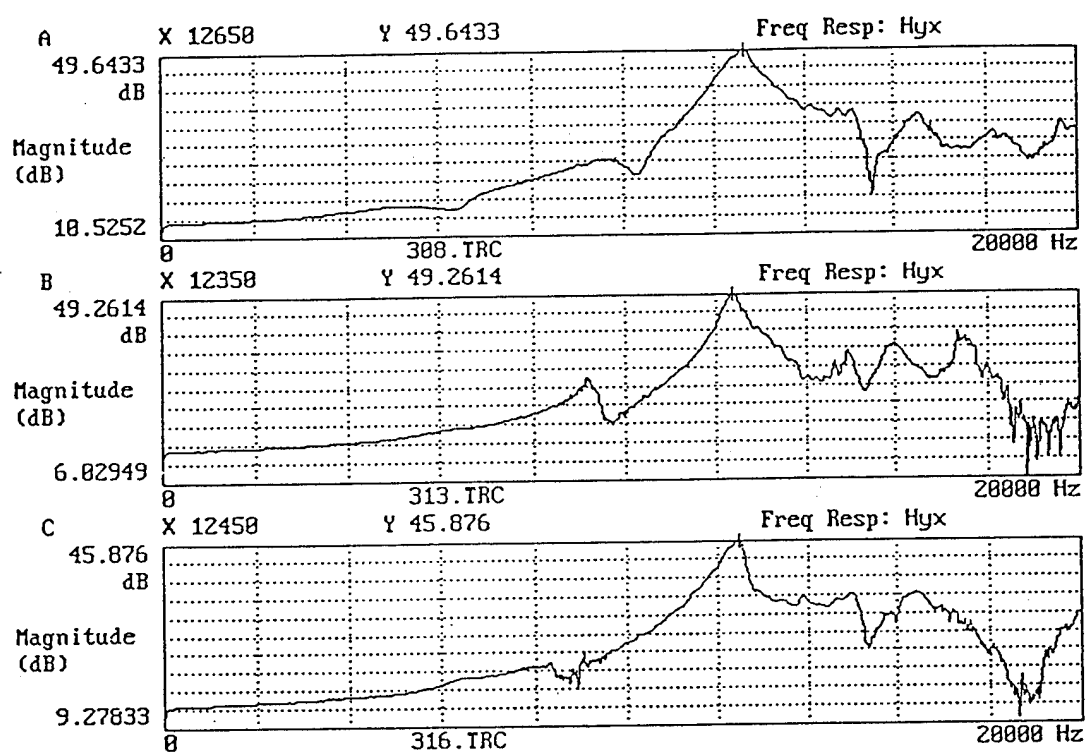**Figure 21.** (Three-segment example) Frequency response trace for 9" x 3" specimen.

Figure 22. (Four-segment example) Frequency response trace for 9" x 3" specimen.